

# Tapping-mode atomic force microscopy and phase-imaging in higher eigenmodes

Robert W. Stark, Tanja Drobek, and Wolfgang M. Heckl<sup>a)</sup>

Universität München, Institut für Kristallographie and Angewandte Mineralogie, Theresienstrasse 41, 80333 München, Germany

(Received 5 January 1999; accepted for publication 1 April 1999)

Tapping-mode atomic force microscopy (TM-AFM) is a powerful tool to study soft biological samples. Higher eigenmodes of the vibrating cantilever offer enhanced signal and smaller time constants increasing the sensitivity of the tapping probe as compared to conventional TM-AFM. The first five eigenmodes of a  $v$ -shaped silicon cantilever were investigated with respect to their suitability for imaging. Stable imaging was possible in the first and third modes. Phase imaging in the third mode was extremely sensitive to surface inhomogeneities and surface contamination particles not visible in standard TM-AFM. © 1999 American Institute of Physics. [S0003-6951(99)01222-X]

Atomic force microscopy (AFM) has become a powerful tool for surface analysis since its invention in 1986.<sup>1</sup> Miscellaneous operation modes are available, addressing different material properties like adhesion, stiffness,<sup>2,3</sup> and chemical composition.<sup>4</sup> In tapping mode AFM the probing tip is in periodic contact with the specimen,<sup>5</sup> reducing the potentially destructive lateral forces. The phase shift between the driving force and the tapping movement of the cantilever gives additional information about the sample surface.<sup>6</sup> However, interpretation of this phase-imaging data is still controversially discussed in literature.<sup>7-11</sup>

The sensitivity is a crucial point in tapping mode AFM. Especially in biological applications it is desirable to keep the energy transferred into the sample to a minimum in order to avoid degradation of the sample. Unwanted hard tip sample interaction is a source for contamination in nanoextraction experiments, where small amounts of DNA are extracted from human chromosomes for diagnostic purposes.<sup>12,13</sup> Furthermore, a desirable quality of AFM imaging is the detection of even the smallest surface inhomogeneities, which is important in semiconductor fabrication. The enhancement of the sensitivity of tapping mode AFM through the usage of higher eigenmodes was investigated by Houmady *et al.*<sup>14</sup> With a piezoresistive cantilever, Minne *et al.*<sup>15</sup> obtained topographic images at a higher mode.

Here, the principal suitability of higher eigenmodes for imaging is investigated. The focus is on differences in the image contrast in phase imaging between different vibrational modes.

A resonance spectrum of a freely vibrating  $v$ -shaped cantilever<sup>16</sup> was recorded for both signals, normal and lateral force, as shown in Fig. 1. Data were obtained with a modified commercial AFM<sup>17</sup> in ambient conditions. In all experiments described here, the identical cantilever was employed. The cantilever was excited by direct modulation of the  $z$  scanner with a typical modulation amplitude of 50 mV.<sup>18</sup> The signal of the quadrant photodiode was demodulated with a lock-in amplifier.<sup>18</sup> The rms amplitude was used as a feed-

back signal. The cross talk between the normal and lateral signal is caused mainly by imperfect photodiode adjustment and by electronic cross talk in the photodiode itself.

To interpret the resonance spectrum a finite element analysis was carried out.<sup>19</sup> The natural modes were calculated by solving the eigenvalue problem:

$$\mathbf{M}\ddot{\mathbf{q}} + \mathbf{K}\mathbf{q} = \mathbf{0}, \quad (1)$$

$\mathbf{M}$  and  $\mathbf{K}$  are the mass and the stiffness matrix, the vector  $\mathbf{q}$  denotes the nodal translation vector. The material parameters are Young's modulus of silicon  $E_{100} = 129.2$  GPa, Poisson ratio  $\nu = 0.28$ ,<sup>20</sup> and mass density  $\rho = 2.33$  g/cm<sup>3</sup>. The cantilever geometry was adjusted slightly within the limits given by the manufacturer to match the measured resonant frequencies. The results are the modal shapes shown in Fig. 2 and the eigenfrequencies of the undamped system given in Table I.

In the symmetric modes (No. 1, No. 3, and No. 5) the tip oscillates vertically as indicated by the arrows, whereas in

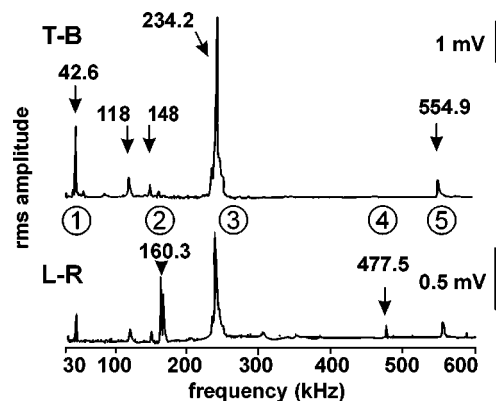


FIG. 1. Frequency response of the free cantilever. Both photodiode signals, top minus bottom reflecting normal bending (above) and left minus right, i.e., the torsion (below) were recorded separately. The natural modes of the cantilever were identified by finite element analysis as indicated. The resonances at 118.1 and 148.1 kHz are electronic noise of the experimental setup. The amplitude is the rms voltage measured by the lock-in amplifier. There is a damping for frequencies larger than 50 kHz due to limited bandwidth of the AFM preamplifier.

<sup>a)</sup>Electronic mail: w.heckl@lrz.uni-muenchen.de

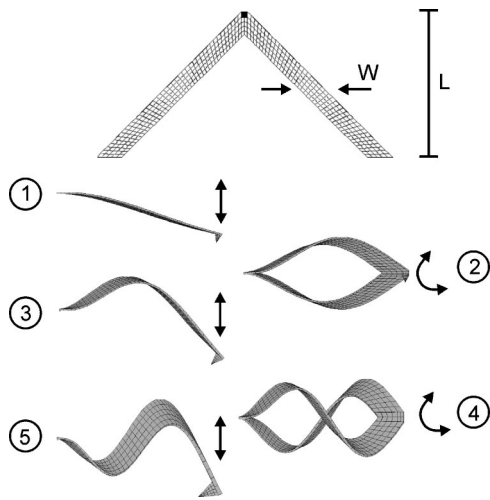


FIG. 2. Cantilever geometry with the mesh used for finite element analysis (above) and the first five eigenmodes obtained for a freely vibrating cantilever (below). The symbols indicate the mode numbers in the sequence of their respective eigenfrequency. The first, third, and fifth mode are symmetric, whereas the second and fourth mode are antisymmetric. The direction of the tip oscillation is indicated by arrows.

both antisymmetric modes (No. 2 and No. 4) the tip vibrates laterally. The sensitivity of the symmetrically oscillating cantilever with respect to the tip sample separation depends on the frequency shift induced by the transition of the freely vibrating (tapping) cantilever to a clamped-sliding configuration. There, the tip is in permanent contact with the surface, but it is allowed to slide on the sample surface. The resonant frequency is dramatically increased [Table I (No. 1, No. 3, and No. 5)]. The antisymmetric modes can be examined by limiting the lateral degree of freedom of the nodes at the tip apex. This represents a tip which is exposed to high shear or frictional forces. The frequency shift as compared to the free cantilever is only less than 20% [Table I (No. 2 and No. 4)]. This implies that torsional vibrating cantilevers are not suited for distance regulation.

Stable topographic and phase imaging could be obtained routinely in the fundamental (No. 1) mode as shown in Figs. 3(a)–3(c). The phase image [Fig. 3(c)] exhibits a contrast between the chemically etched SiO<sub>2</sub> on the table like structures and the Si on the base (phase contrast:  $\Delta\phi = 13.7^\circ$ ), which is covered by a thin natural oxide layer. The contrast is induced by the different elastic moduli in the bulk as the chemical composition on the surface is similar. As expected, both antisymmetric vibrational modes (No. 2 and No. 4) did not yield stable imaging conditions. The third mode (No. 3) allowed routine imaging as shown in Figs. 3(d)–3(f). The

TABLE I. Eigenfrequencies of the cantilever obtained by finite element analysis in different configurations. The “free” system reflects an oscillating cantilever without contact to the sample (see Fig. 2). Restricted systems are modeled by limitation of translational degrees of freedom  $u$  of the nodes at the tip apex. The configuration  $u_z = 0$  represents a frictionless sliding tip in contact with the sample. The frequency shift of an antisymmetric vibrating cantilever can be estimated with  $u_x = 0$ , a laterally confined tip.

Restriction	$f_1$ (kHz)	$f_2$ (kHz)	$f_3$ (kHz)	$f_4$ (kHz)	$f_5$ (kHz)
free	41.7	164.2	232.7	507.7	578.0
$u_z = 0$	151.9	164.2	451.8	507.7	934.2
$u_x = 0$	41.7	199.0	232.7	566.5	578.0

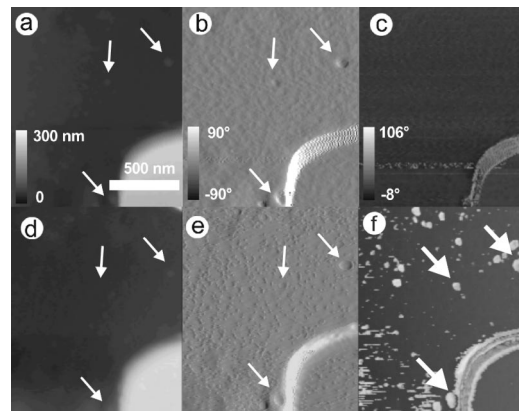


FIG. 3. AFM images of a test structure in the fundamental (above) and third (below) eigenmode. The sample consists of crystalline Si with a natural oxide layer. The table like structures are chemically etched SiO<sub>2</sub>. The arrows point to surface inhomogeneities. The topography and its derivative in the fundamental mode (a),(b) are similar to the corresponding data obtained in the third mode (d),(e). The phase image in the fundamental mode (c) reflects the different elastic properties of Si ( $E_{100} = 129.2$  GPa) and SiO<sub>2</sub> ( $E = 40\text{--}90$  GPa). The phase image obtained in the third mode strongly enhances small contamination structures. (Scaling and color scheme of the corresponding images are equal.)

operating setpoint was in the repulsive regime, well below the transition to the attractive regime. A comparison of the derivatives of the topographic images [Figs. 3(b) and 3(e)] demonstrates that even small features are imaged with comparable resolution. However, the phase image in the third mode [Fig. 3(f)] differs significantly from the phase image in the fundamental mode [Fig. 3(c)]. Several surface inhomogeneities become prominent (arrows) which are difficult to be distinguished in the topographic image. Reduction of the setpoint did not change the phase contrast. The phase contrast changed when the AFM was operated in the attractive range. The material contrast disappeared and a topography induced contrast pronouncing the derivative of the topography was visible (data not shown). In the fifth mode imaging was not possible. Although this mode is symmetric, imperfections in the cantilever geometry can give rise to uncontrolled cantilever oscillations, which prevent a stable feedback. It is worth noting that the choice of the cantilever type is a critical point in this experiment. There are commercially available Si<sub>3</sub>N<sub>4</sub> cantilevers where modes No. 2 and No. 3 nearly coincide.<sup>21</sup> Then, stable imaging cannot be expected in mode No. 3.

It is astonishing that such differences in the phase contrast between both eigenmodes (No. 1 and No. 3) occur. In Refs. 10 and 11 the contrast in phase imaging is discussed in the light of energy dissipation through tip–sample interaction. In addition to the process discussed there, another dissipation mechanism might become significant. The periodic force acting to the free end of the cantilever induced by the tapping tip can give rise to an excitation of a higher eigenmode with an eigenfrequency beyond the detection limit of the experiment. This resonant excitation requires that the eigenfrequency of the higher mode is an integer multiple of the original driving frequency.<sup>22</sup> The degree of these anharmonic contributions depends on the sample stiffness.<sup>23</sup> As a result, the phase image might be a very sensitive map of the degree of cross talk to higher modes enhancing loosely

bound particles on the specimen. It is evident that the requirement to match the eigenfrequencies of at least two modes imposes restrictions on the driving frequency and the cantilever used.

In summary, the first five vibrational modes of a *v*-shaped cantilever were investigated with respect to their suitability for tapping mode or noncontact mode AFM. Antisymmetric modes turned out to be too insensitive to the tip sample separation for imaging. The symmetric modes are suited in principle for imaging purposes. In the third eigenmode, imaging could be performed routinely. In the phase-signal, surface inhomogeneities became prominent which were not visible in conventional tapping mode or phase imaging AFM. These contaminations can have important consequences for the performance of semiconductors or optical devices. Tapping mode AFM together with phase imaging in higher eigenmodes has the potential to detect these imperfections.

The authors thank Physik Instrumente GmbH Germany for supplying the lock-in amplifier for test purposes, G. Schrag and P. Scheubert (Technische Universität München, Germany) for the introduction into ANSYS. This work was supported by Bayerische Forschungstiftung and DFG Grant No. He-1617/7-1.

<sup>1</sup>G. Binnig, C. F. Quate, and C. Gerber, *Phys. Rev. Lett.* **56**, 930 (1986).

<sup>2</sup>M. Radmacher, M. Fritz, and P. K. Hansma, *Biophys. J.* **69**, 264 (1995).

<sup>3</sup>R. W. Stark, T. Drobek, M. Weth, J. Fricke, and W. M. Heckl, *Ultramicroscopy* **75**, 161 (1998).

<sup>4</sup>C. D. Frisbie, L. F. Rozsnyai, A. Noy, M. S. Wrighton, and C. M. Lieber, *Science* **265**, 2071 (1994).

<sup>5</sup>Q. Zhong, D. Inness, K. Kjoller, and V. B. Elings, *Surf. Sci. Lett.* **290**, L688 (1993).

<sup>6</sup>S. N. Magonov, V. Elings, and M. H. Whangbo, *Surf. Sci. Lett.* **375**, L385 (1997).

<sup>7</sup>R. G. Winkler, J. P. Spatz, S. Sheiko, M. Möller, P. Reineker, and O. Marti, *Phys. Rev. B* **54**, 8908 (1996).

<sup>8</sup>J. Tamayo and R. García, *Langmuir* **12**, 4430 (1996).

<sup>9</sup>N. A. Burnham, O. P. Behrend, F. Ouvevey, G. Gremaud, P. J. Gallo, D. Gourdon, E. Dupas, A. J. Kulik, H. M. Pollock, and G. A. D. Briggs, *Nanotechnology* **8**, 67 (1997).

<sup>10</sup>J. P. Cleveland, B. Anczykowski, A. E. Schmid, and V. B. Elings, *Appl. Phys. Lett.* **72**, 2613 (1998).

<sup>11</sup>J. Tamayo and R. García, *Appl. Phys. Lett.* **73**, 2926 (1998).

<sup>12</sup>S. Thalhammer, R. W. Stark, S. Müller, J. Wienberg, and W. M. Heckl, *J. Struct. Biol.* **119**, 232 (1997).

<sup>13</sup>R. W. Stark, S. Thalhammer, J. Wienberg, and W. M. Heckl, *Appl. Phys. A: Mater. Sci. Process.* **66**, S579 (1998).

<sup>14</sup>M. Houmady and E. Farnault, *Appl. Phys. A: Mater. Sci. Process.* **66**, S361 (1998).

<sup>15</sup>S. C. Minne, S. R. Manalis, A. Atalar, and C. F. Quate, *Appl. Phys. Lett.* **68**, 1427 (1996).

<sup>16</sup>Uncoated silicon cantilever SC 11, nominal spring constant  $k=3.0$  N/m, eigenfrequency  $f_0=40$  kHz,  $L=200$   $\mu\text{m}$ ,  $W=40$   $\mu\text{m}$ ,  $T=2.0$   $\mu\text{m}$  (NT-MDT, Russia).

<sup>17</sup>Topometrix Explorer, 130  $\mu\text{m}$  dry scanner (Topometrix GmbH, Darmstadt, Germany).

<sup>18</sup>Function generator DS 345 and lock-in amplifier SR 844, Stanford Research Systems.

<sup>19</sup>ANSYS 5.4 running on an IBM SP2 workstation at the Leibnitz Rechenzentrum, München, Germany.

<sup>20</sup>Landolt-Börnstein, edited by K. H. Hellwege and A. M. Hellwege, New York (1979), p. 11.

<sup>21</sup>T. Drobek, R. W. Stark, M. Gräber, and W. M. Heckl (unpublished).

<sup>22</sup>This can be verified by Fourier transformation.

<sup>23</sup>J. P. Hunt and D. Sarid, *Appl. Phys. Lett.* **72**, 2969 (1998).